Estimation of PWC gradients over the Kanto Plain using GPS data: Validation and possible meteorological implications

Kazumasa Aonashi[1], Yoshinori Shoji[1], Ryu-ichi Ichikawa[2], and Hiroshi Hanado[3]

[1]*Meteorological Research Institute, Nagamine 1-1, Tsukuba-shi, Ibaraki 305-0052, Japan*
[2]*Kashima Space Communication Center, Communication Research Laboratory, Hirai 893-1, Kashima-shi, Ibaraki 314-0012, Japan*
[3]*Communication Research Laboratory, Nukui-Kitamachi 4-2-1, Koganei-shi, Tokyo 184-0015, Japan*

(Received December 29, 1999; Revised August 3, 2000; Accepted August 9, 2000)

Simultaneous GPS and water vapor radiometer (WVR) observations were carried out in Tsukuba during May–June 1998, for the validation of precipitable water content (PWC) gradients estimated from single-site GPS data. Slant path PWC observed by WVR were fitted into hourly PWC gradients (WVR gradients) using the least-square method. GPS PWC gradients were retrieved from tropospheric delay gradients that were estimated with GIPSY OASYS 2 package (GIPSY gradients). The results indicate that GIPSY gradients had good, linear correlation with WVR gradients, especially for a large gradient range. Both gradients had spike-shaped, short time-scale (∼3 hours) peaks which were mostly associated with synoptic fronts. The GIPSY gradients were also compared with meso-scale PWC gradients calculated from zenith wet delay data of GPS network (NET gradients). The results show that GIPSY gradients did not have very good correlation with NET gradients, and that significant meso-scale discrepancy existed between the two gradients for a cold frontal case on 19 June 1998. One possible reason for this discrepancy is vertical differences in RH gradients, because GIPSY gradients are sensitive to RH gradients around the scale height of humidity (∼2500 m) while RH gradients in lowermost level have largest weights for NET gradients. To study PWC gradients associated with the fronts, GPS gradients were compared with other meteorological data over the Kanto Plain for two frontal cases. The results indicate that large PWC gradient zones with horizontal scale of about several tens kilometers in cross-frontal directions were collocated with the surface wind shear zones of the fronts. This suggests that the large PWC gradients were due to humidity discontinuity around the fronts.

1. Introduction

Global Positioning System (GPS) has vast potential as a meteorological sensor as well as geodetic instrument. Bevis *et al.* (1992), Rocken *et al.* (1993), and other studies indicated that precipitable water content (PWC) is accurately retrieved from GPS signals. Recent studies, such as Ruffini *et al.* (1999), have shown that local-scale (∼10 km) PWC gradients can also be estimated from single-site GPS data.

From accurate PWC gradient data with meso-scale (several tens kilometers) resolution, we can retrieve fine structure of humidity distribution that is not resolvable with sparse, conventional humidity observation networks. Accordingly, GPS-derived PWC gradients data are very important as input to meso-scale meteorological analysis and numerical weather prediction.

The objective of this study is to validate the accuracy of GPS PWC gradients and to know relationship between PWC gradients and meteorological disturbances. For the statistical validation of single-site GPS PWC gradients, we carried out simultaneous GPS and water vapor radiometer (WVR) observation in Tsukuba, northeastern part of the Kanto Plain, during May–June 1998. The single-site GPS PWC gradients were also compared with meso-scale PWC gradients calculated from zenith wet delay data of GPS network in the Kanto Plain where mountainous influence on GPS observation can be neglected. The results indicate that single-site GPS PWC gradients had high, linear correlation with the WVR-derived PWC gradients, while correlation between single-site and meso-scale gradients were not very good.

To study PWC gradients associated with meteorological disturbances, we compared GPS PWC gradients with other meteorological observation data for this period (May–June 1998) over the Kanto Plain. It is found that large PWC gradient zones with horizontal scale of about several tens kilometers in cross-frontal directions were collocated with the surface wind shear zones of synoptic fronts.

2. Estimating PWC Gradients

2.1 PWC gradient estimation from WVR data

To obtain reference data for GPS PWC gradients, we observed PWC along slant paths with a ground-based WVR, and estimated local-scale PWC gradients from the slant path PWC. In this section, we describe the WVR observations and the estimation procedures of WVR PWC gradients.

We performed WVR observations using a dual frequency (23.8 and 31.4 GHz) WVR at Meteorological Research Institute (MRI) in Tsukuba during 11 May through 30 June 1998. With this instrument, we observed downward atmospheric microwave radiation in the vertical direction and along 12 slant paths with elevation angle (θ) of 20 degree. Azimuths

(ϕ) of each slant paths were set from 0 to 330 degree at interval of 30 degree. From the microwave radiation, we retrieved PWC using the Radiometrics algorithm (Radiometrics Corp., 1998).

To validate the accuracy of WVR PWC, we compared the vertical WVR PWC observations at 00 and 12 UTC during May–June 1998 with PWC calculated from operational sonde observations in Tsukuba. The results show that WVR PWC agreed well with the sonde PWC with root-mean-square (RMS) error of 2.08 kg m^{-2} and linear correlation coefficient of 0.975, for rain-free cases. Microwave radiation from rain drops degraded WVR PWC accuracy when large amount (>0.3 kg m^{-2}) of vertical liquid water content (LWC) was retrieved. Based on this result, we exclude slant path PWC if LWC along the path exceeds 0.3 secθ kg m^{-2} to avoid rain contamination of WVR PWC. About 26% of the slant path PWC data during the observation period were rejected by this rain contamination check.

We derive information on spatial humidity gradients from slant path PWC. PWC along a slant path (ϕ, θ) (SPWC(ϕ, θ)) can be written in the following form:

$$\begin{aligned}\mathrm{SPWC}(\phi,\theta) &= m(\theta)\int \rho_v(x,y,z)dz \\ &= m(\theta)\int \rho_v(z\cot\theta\sin\phi, z\cot\theta\cos\phi, z)dz, \quad (1)\end{aligned}$$

where ρ_v is the specific humidity, $m(\theta)$ is the mapping function. In this study, sec θ is adopted as $m(\theta)$ for Eq. (1). Using Taylor expansion, SPWC(ϕ, θ) is approximated as follows:

$$\begin{aligned}\mathrm{SPWC}(\phi,\theta) \approx m(\theta)&\int \rho_v(0,0,z)dz \\ &+ m(\theta)\int \frac{\partial\rho_v}{\partial x} z\cot\theta\sin\phi \\ &+ \frac{\partial\rho_v}{\partial y} z\cot\theta\cos\phi dz. \quad (2)\end{aligned}$$

Introducing a gradient vector $\bar{G}_{\mathrm{pwc}}$: $\bar{G}_{\mathrm{pwc}}$

$$= \left(\int \frac{\partial\rho_v}{\partial x} z dz, \int \frac{\partial\rho_v}{\partial y} z dz\right), \quad (3)$$

we can rewrite Eq. (2) in the following form:

$$\mathrm{SPWC}(\phi,\theta) \approx m(\theta)\mathrm{PWC} + m(\theta)(\bar{G}_{\mathrm{pwc}}, \bar{e}_\phi)\cot\theta, \quad (4)$$

where $\bar{e}_\phi = (\cos\phi, \sin\phi)$ is the azimuth unit vector. Using Eq. (4), we estimated hourly $\bar{G}_{\mathrm{pwc}}$ from slant path PWC observations by least square fitting method.

To calculate PWC gradients from $\bar{G}_{\mathrm{pwc}}$, we assume that gradients in relative humidity (RH) are constant in the vertical. Based on this assumption, $\bar{G}_{\mathrm{pwc}}$ is approximated as follows:

$$\begin{aligned}\bar{G}_{\mathrm{pwc}} &= \left(\frac{\partial\mathrm{RH}}{\partial x}, \frac{\partial\mathrm{RH}}{\partial y}\right)\int \rho_{vs} z dz \\ &= \left(\frac{\partial\mathrm{RH}}{\partial x}, \frac{\partial\mathrm{RH}}{\partial y}\right)\mathrm{PWC}_{sat} Z_{vs} \\ &= \left(\frac{\partial\mathrm{PWC}}{\partial x}, \frac{\partial\mathrm{PWC}}{\partial y}\right) Z_{vs}, \quad (5)\end{aligned}$$

where ρ_{vs} is the saturated specific humidity, PWC_{sat} is PWC of the saturated air, Z_{vs} is a scale height of humidity that is defined as follows: $Z_{vs} = \int \rho_{vs} z dz / \int \rho_{vs} dz$.

In this study, Z_{vs} is determined as 2500 m, based on operational sonde observations in Tsukuba during May–June 1998. Hereafter these gradients are referred to as WVR gradients.

To evaluate the detective range of the WVR PWC gradients, we consider PWC difference between slant paths along opposite directions (dPWC). If dPWC is larger than the accuracy of WVR PWC (2.08 kg m^{-2}), we are confident that there exists PWC gradient in this direction. Using Eqs. (4) and (5), PWC gradient in this direction (∇PWC) can be written in terms of dPWC in the following form:

$$\nabla\mathrm{PWC} \approx \mathrm{dPWC}\sin\theta/(2Z_{vs}). \quad (6)$$

Substitution of dPWC of 2.08 kg m^{-2} to this equation yields ∇PWC of 0.142 kg m^{-2} km^{-1}. Accordingly, we are not confident in WVR gradient if its amplitude is smaller than 0.142 kg m^{-2} km^{-1}.

2.2 PWC gradient estimation from single-site GPS data

We estimated local-scale PWC gradients from atmospheric delay observations along slant paths between one GPS site and GPS satellites. In this section, we describe the estimation procedures using single-site GPS data.

We deployed an Ashtech Z-12 GPS receiver at MRI for May–June 1998. This receiver was operated with an elevation cut-off angle of 5 degree and a sampling rate of 10 second during the observation period. Because of the constellation of GPS satellites, azimuths and elevation angles of the slant paths are widely distributed.

The GIPSY OASYS 2 package was used with a precise point positioning strategy to analyze the GPS data. (The details are described by Shoji *et al.* (2000).) In the analysis, the atmospheric delay along a slant path ($L(\phi, \theta)$) is modeled (MacMillan, 1995) as:

$$L(\phi,\theta) \approx m(\theta)Lz + m(\theta)(\bar{G}_L, \bar{e}_\phi)\cot\theta, \quad (7)$$

where Lz is the atmospheric zenith delay, $\bar{G}_L$ is a gradient vector of the atmospheric delay. Using this software, we estimate hourly average of Lz and $\bar{G}_L$ from $L(\phi, \theta)$ with wide ranges of azimuths and elevation angles.

To obtain a gradient vector of the wet atmospheric delay, we assume that $\bar{G}_L$ is equal to the wet atmospheric delay gradients, neglecting the dry gradient components. This is because water vapor has much higher local-scale variability than dry air.

Then, we converted $\bar{G}_L$ into $\bar{G}_{\mathrm{pwc}}$ using a conversion coefficient (Π) from the wet atmospheric delay to PWC. In this study, we calculate Π, adopting Ohtani *et al.* (1997)'s method that statistically determined Π as a function of temperature and pressure at the surface level.

To estimate hourly-averaged PWC gradients from the GPS-derived $\bar{G}_{\mathrm{pwc}}$, we adopt Eq. (5) using the same value of Z_{vs} as Subsection 2.1. Hereafter these gradients are referred to as GIPSY gradients.

2.3 Meso-scale PWC gradient estimation from GPS network

To obtain meso-scale PWC gradients around Tsukuba, we used GPS data of Geographical Survey Institute (GSI) GPS

network (GEONET) whose horizontal resolution is about 20 km over the Kanto Plain. Hourly Lz is retrieved from the GEONET GPS data with GIPSY software. Then we converted Lz into PWC using the same procedures as Subsection 2.2. We calculate PWC gradients by taking horizontal differentiation of GEONET PWC pattern (hereafter referred to as NET gradients).

3. Validation of the PWC Gradients

We compared the WVR and GIPSY gradients at MRI for 11 May–30 June 1998. Scatter diagrams between the two data sets (Fig. 1) indicate that the GIPSY gradients have good, linear correlation with the WVR gradients, especially for large gradient ranges. Linear correlation coefficients and RMS differences between the two gradients are 0.531 and 0.0573 kg m^{-2} km^{-1} for east-west direction, 0.748 and 0.0576 kg m^{-2} km^{-1} for north-south direction, respectively. The correlation is higher for north-south components that had larger amplitudes of PWC gradients compared to east-west components. This result is consistent with the discussion in Subsection 2.1 that pointed out the difficulty in estimating weak PWC gradients with single-site slant-path PWC.

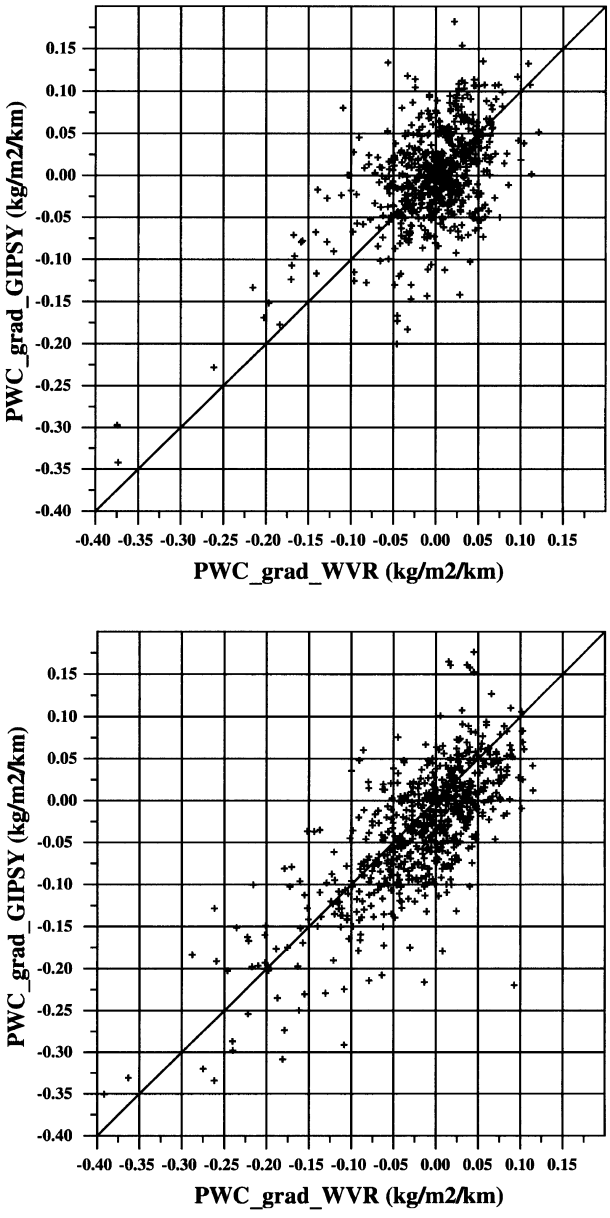

Fig. 1. Scatter diagrams between WVR and GIPSY gradients (kg m^{-2} km^{-1}) at MRI during 11 May–30 June 1998. (a) East-west component. (b) North-south component.

The time sequence of the gradients indicates that both gradients had spike-shaped, short-time-scale (∼3 hours) peaks at the same time. Most of the peaks were associated with synoptic fronts, while some were caused by local disturbances. This coincidence is one reason why both gradients had high statistical correlation. For periods with PWC gradients smaller than 0.1 kg m^{-2} km^{-1}, GIPSY gradients did not agree well with WVR gradients because of the difficulty in estimating weak PWC gradients.

The GIPSY gradients were also compared with NET gradients around Tsukuba for 11 May–30 June 1998. The results show that correlation coefficients between the two data sets (0.296 for east-west and 0.321 for north-south direction) are much poorer than those between the GIPSY and WVR gradients.

4. Comparison between GIPSY Gradients and Other Meteorological Data for Frontal Cases

4.1 Data used in the comparison

We retrieved PWC and PWC gradients from GEONET data over Kanto using the method described in Subsection 2.2.

For meteorological data, we used surface wind and temperature data that were provided by the Japan Meteorological Agency (JMA) automated surface meteorological observation system (AMeDAS). The horizontal resolution of AMeDAS sites are almost equivalent to that of GEONET GPS sites. We also used hourly precipitation analysis data that were retrieved from JMA's radar and surface rain gauge data. (The details are described by Makihara *et al.* (1995).)

4.2 Stationary (Baiu) frontal case (24 June 1998)

A stationary (Baiu) front with east-southeast direction passed over Kanto during 23–24 June 1998. Figure 2(a) presents surface wind, surface temperature, GEONET PWC, and hourly precipitation for 06 UTC 24 June. A horizontal wind shear zone was found between an east-southeasterly wind in central Kanto and a southerly wind in southwestern Kanto. To northeast of the shear zone, large spatial variation of GEONET PWC existed in the cross-front (north-northeast) direction. Surface temperature had small changes for this case, except for mountain areas in northern Kanto. Those weak temperature gradients are typical of the Baiu front.

As Figs. 2(b) and (c) show, GIPSY gradients agreed well with NET gradients in this case. A large PWC gradient zone was retrieved in central Kanto from both gradient data. This large gradient zone had horizontal scale of about several ten kilometers in north-northeast (cross-front) direction and of about 200 km in east-southeast (along-front) direction.

Comparing the GIPSY gradients with the meteorological data, we found that the meso-scale, large GIPSY gradient zone was located to a few kilometers northeast of the horizontal wind shear zone along the stationary front. Thus we consider that this large GIPSY gradient zone means meso-

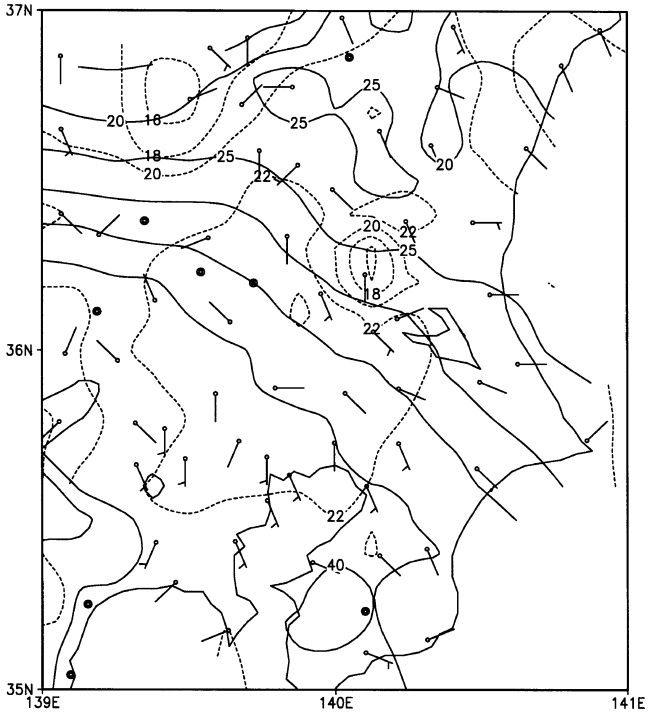

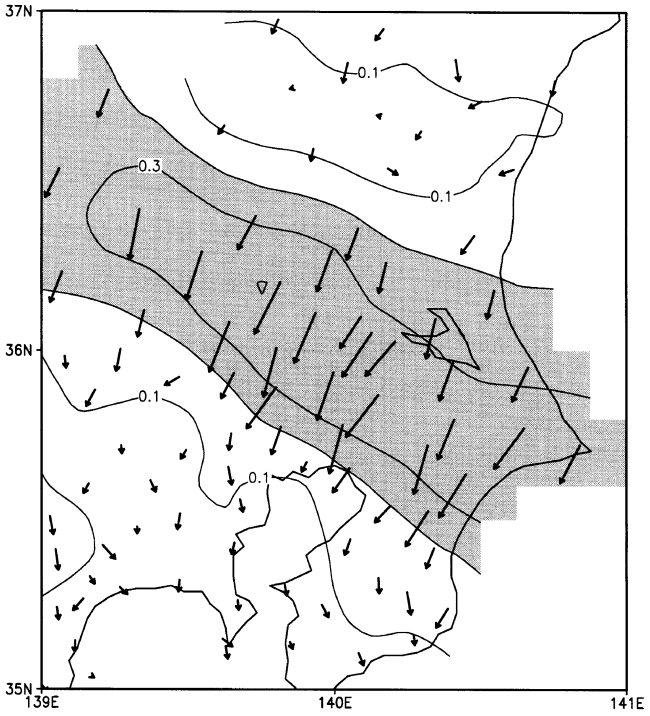

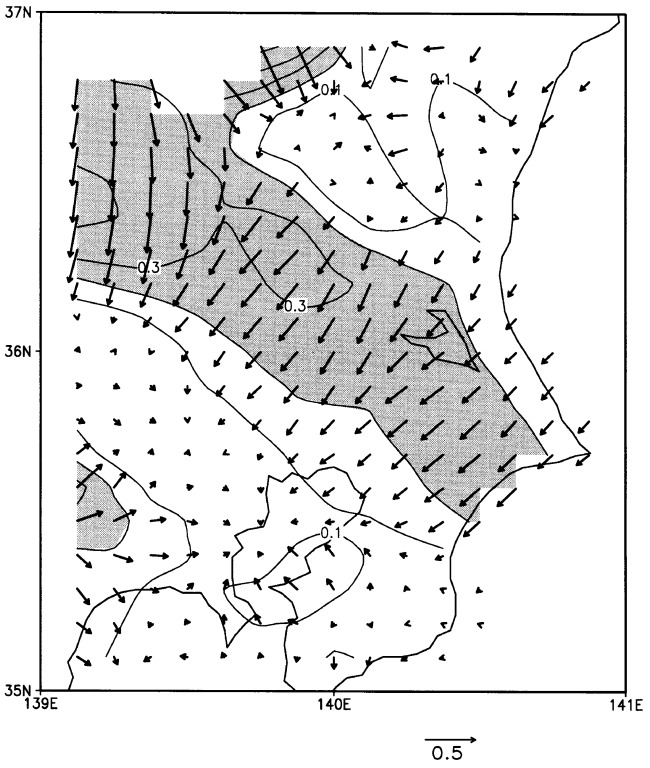

Fig. 2. Comparison between GIPSY gradients and other meteorological data for 06 UTC 24 June. (a) Surface wind (barbs), surface temperature (dashed lines), hourly precipitation (shade), and GEONET PWC distribution (solid lines) over Kanto for 06 UTC 24 June. A half and a full barb represent 5 m s^{-1} and 10 m s^{-1}, respectively. Solid lines are at every 5 kg m^{-2}. Dashed lines are at every 2 C. Areas with hourly precipitation over 0.5 mm hr^{-1} are shaded. (b) NET gradients over Kanto for 06 UTC 24 June. Arrows and contours represent the gradient vectors and their amplitudes. Contours are at every 0.1 kg m^{-2} km^{-1}. Areas with the amplitude over 0.2 kg m^{-2} km^{-1} are shaded. (c) Same as Fig. 2(b) but for GIPSY gradients.

Fig. 2. (continued).

scale humidity discontinuity around the front.

4.3 Cold frontal case (19 June 1998)

A cold front with northeast direction moved over Kanto during 19–20 June 1998. Figure 3(a) shows the meteorological data for 18 UTC 19 June. There existed a horizontal wind shear zone between a southwesterly wind in southeast Kanto and a weak wind area in northwest Kanto. We also found a surface temperature front along this shear zone. GEONET PWC pattern, however, showed small changes around the boundary.

To investigate the cause of this difference between the temperature and PWC patterns, we checked the meteorological data before this time (figures not shown). We found that precipitation occurred over the Kanto Plain during 03–16 UTC while only very weak precipitation was observed at 18 UTC. Thus, it is considered that low-level atmosphere was moisten and cooled by precipitation, and that the wet air was pooled in the northwestern part of Kanto.

Figure 3(b) shows NET gradient at this time. PWC gradients were small over Kanto Plain, reflecting the small variability of GEONET PWC. Large PWC gradient was confined in northwestern and western edges of the Kanto Plain. In this case, we did not found any apparent changes in NET gradients in the vicinity of the wind shear zone.

Figure 3(c) shows GIPSY gradients for this case. Contrary to the stationary frontal case, there existed significant differences from NET gradients. GIPSY gradients were much stronger than NET gradients over Kanto Plain. For example, GIPSY gradients in Tsukuba had about 3 times as large amplitude as NET gradients. Areas with GIPSY gradient larger than 0.3 kg m^{-2} km^{-1} were found in west to north part of Kanto. It is also noteworthy that the GIPSY gradients

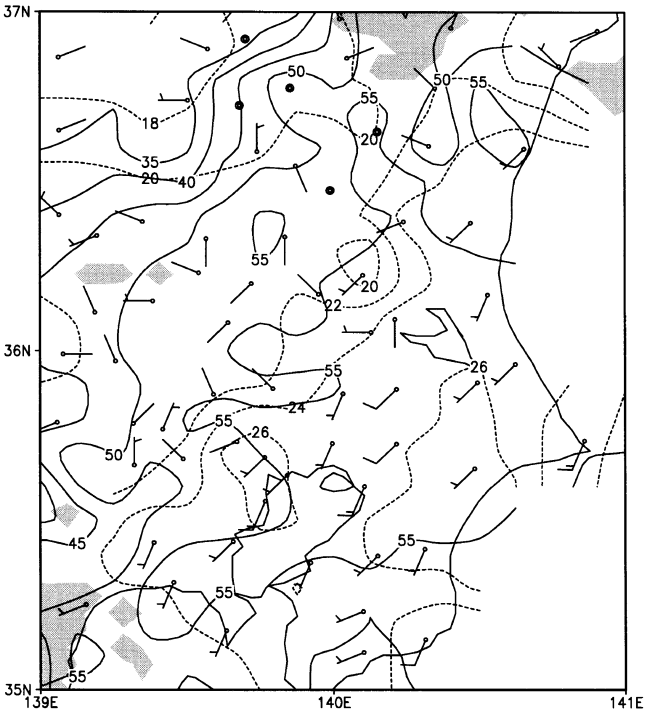

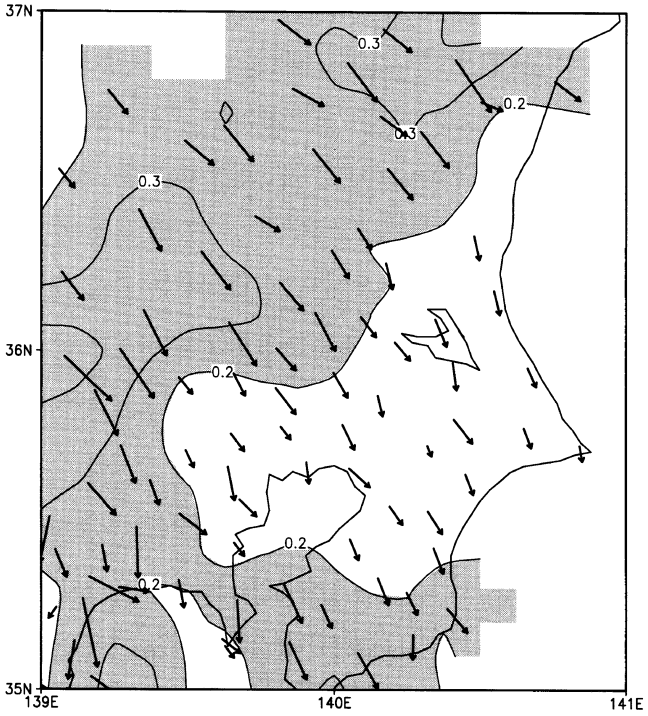

Fig. 3. (continued).

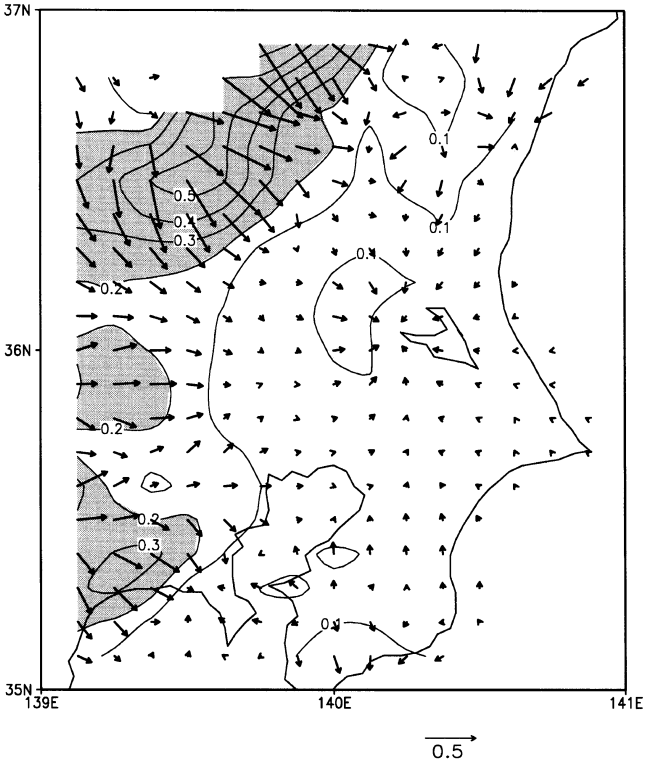

Fig. 3. Same as Fig. 2 but for 18 UTC 19 June.

had southeast direction all over the Kanto Plain where NET gradients had various directions.

The large GIPSY gradient zone in northwest Kanto was located to a few kilometers northwest of the wind shear zone and the large temperature change along the cold front. Hence, this large gradient is considered as humidity discontinuity that is expected in the cross-front direction.

5. Discussion

In this study, we retrieved PWC gradients using WVR and GPS data in Tsukuba during May–June 1998. The results show that GIPSY gradients had good, linear correlation with WVR gradients, similar to the previous studies, such as Ruffini *et al.* (1999). These PWC gradients also have the maximum amplitudes ($\sim$0.5 kg m^{-2} km^{-1}) like those reported by Ruffini *et al.* (1999) and MacMillan (1995).

In estimating WVR and GIPSY gradients, we derived the gradient vectors of PWC from single-site WVR and GPS observations along slant paths. Then, we estimated both WVR and GIPSY gradients using the same procedures, assuming the constant profile of RH gradients and prescribed scale height of humidity. Accordingly, the good results indicate that atmospheric wet delays can be accurately retrieved along slant paths from GPS data.

In addition to the validation with WVR gradients similar to Ruffini *et al.* (1999), we also compared GIPSY gradients with NET gradients that presented meso-scale PWC variation over Kanto Plain. As the results, we found that correlation between the two data sets was much poorer than those between the GIPSY and WVR gradients. As discussed in Subsection 4.3, the discrepancy between the two data sets had a meso-scale systematic structure. Hence, we do not think that this discrepancy was caused by local-scale humidity fluctuation which was not resolved by GEONET.

One possible reason for the discrepancy is vertical difference in RH gradients. We assumed the constant profile of RH gradients in estimating WVR and GIPSY gradients from single-site data. In the real atmosphere, however, RH gradients are not constant in the vertical. Assuming the exponential profile of ρ_v : $\rho_v \approx \rho_0 \mathrm{RH} \exp(-z/Z_{vs})$, we can

approximate Eq. (3) as follows:

$$\bar{G}_{\mathrm{pwc}} = \left(\int \frac{\partial \mathrm{RH}}{\partial x} \rho_0 \exp(-z/Z_{vs}) z dz, \int \frac{\partial \mathrm{RH}}{\partial y} \rho_0 \exp(-z/Z_{vs}) z dz \right). \quad (8)$$

This equation indicates that WVR and GIPSY gradients are most sensitive to RH gradients around Z_{vs}. On the other hand, NET gradients are most sensitive to RH gradients at the lowest level since ρ_v usually has its maximum near the surface level.

If the discrepancy really reflects the vertical difference in RH gradients, it is possible to retrieve humidity profile from GIPSY and NET gradient data. To validate this, we need to compare the GIPSY gradients with high-density experimental observations of humidity profile.

It is also found in this study that large GIPSY gradients were meso-scale phenomena concentrated in time ($\sim$3 hours) and space ($<$100 km). Comparison with other meteorological data indicates that most of the large GIPSY gradients were associated with synoptic fronts, and that these large GIPSY gradients were collocated with horizontal wind shear zones and large temperature variations along the fronts. From the results, we infer that the large GIPSY gradients were due to humidity discontinuity around the fronts. To validate this, the high-density experimental observations are also essential.

6. Conclusions

We carried out GPS and WVR observations in Tsukuba during May–June 1998, for the validation of PWC gradients estimated from single-site GPS data. Slant path PWC observed by WVR were fitted into WVR gradients using the least-square method. GIPSY gradients were retrieved from tropospheric delay gradients that were estimated with GIPSY OASYS 2 package. The results indicate that GIPSY gradients had good, linear correlation with WVR gradients, especially for a large gradient range. Both gradients had spike-shaped, short time-scale ($\sim$3 hours) peaks which were mostly associated with synoptic fronts.

We also compared the GIPSY gradients with NET gradients calculated from zenith wet delay data of GEONET data. The results show that GIPSY gradients did not have very good correlation with NET gradients, and that significant meso-scale discrepancy existed between the two gradients for a cold frontal case on 19 June 1998. One possible reason for this discrepancy is vertical differences in RH gradients, because GIPSY gradients are sensitive to RH gradients around the scale height of humidity, while RH gradients in lowermost level have largest weights for NET gradients.

We compared GPS gradients with other meteorological data over the Kanto Plain for two frontal cases. As the results, we found that large GIPSY gradients were meso-scale phenomena, collocated with horizontal wind shear zones and large temperature variations along the fronts. This suggests that the large GIPSY gradients were due to humidity discontinuity around the fronts.

Acknowledgments. The authors express their thanks to members of "GPS/MET Japan" project, especially Dr. Hajime Nakamura, Mr. Hiromu Seko, Dr. Akinori Ichiki, for their kind cooperation and fruitful discussion, and to staff members of Japan Geographical Survey Institute for providing the GEONET GPS data. This work is a part of "GPS/MET Japan" project financially supported by the Japanese Science and Technology Agency.

References

Bevis, M., S. Businger, T. A. Herring, C. Rocken, R. A. Anthes, and R. H. Ware, GPS Meteorology: Remote sensing of atmospheric water vapor using the Global Positioning System, *J. Geophys. Res.*, **97**, 15787–15801, 1992.

MacMillan, D. S., Atmospheric gradients from very long baseline interferometry observations, *Geophys. Res. Lett.*, **22**, 1041–1044, 1995.

Makihara, Y., N. Kitabatake, and M. Obayashi, Recent development in algorithm for the JMA nowcasting system Part I: Radar echo composition and Radar-AMeDAS precipitation analysis, *The Geographical Magazine, series 2*, **1**(3), 171–204, 1995.

Ohtani, R., H. Tsuji, N. Mannoji, J. Segawa, and I. Naito, Precipitable water vapor observed by geographical survey institute's GPS network, *Tenki*, **44**, 317–325, 1997 (in Japanese).

Radiometrics Corp., "WVR 1100—water vapor and liquid water radiometer", Radiometrics Corp., 32 pp., 1998.

Rocken, C., R. Ware, T. VanHove, F. Solheim, C. Alber, J. Johnson, M. Bevis, and S. Businger, Sensing atmospheric water vapor with the Global Positioning System, *Geophys. Res. Lett.*, **14**, 2631–2634, 1993.

Ruffini, G., L. P. Kruse, A. Rius, B. Burki, L. Cucurull, and A. Flores, Estimation of tropospheric zenith delay and gradients over the Madrid area using GPS and WVR data, *Geophys. Res. Lett.*, **26**, 447–450, 1999.

Shoji, Y., H. Nakamura, K. Aonashi, A. Ichiki, H. Seko, and Members of GPS/MET Japan Summer Campaign 1997 in Tsukuba, Semi-diurnal and diurnal variation of errors in GPS precipitable water vapor at Tsukuba, Japan caused by site displacement due to ocean tidal loading, *Earth Planets Space*, **52**, 685–690, 2000.

K. Aonashi (e-mail: aonashi@mri-jma.go.jp), Y. Shoji, R. Ichikawa, and H. Hanado